Crop Photosynthetic Performance Monitoring Based on a Combined System of Measured and Modelled Chloroplast Electron Transport Rate in Greenhouse Tomato

Wenjuan Yu [1,2], Oliver Körner [2]* and Uwe Schmidt [1]*

[1] Department of Biosystems Engineering, Humboldt University of Berlin, Berlin, Germany, [2] Next-Generation Horticultural Systems, Leibniz-Institute of Vegetable and Ornamental Crops (IGZ), Grossbeeren, Germany

Combining information of plant physiological processes with climate control systems can improve control accuracy in controlled environments as greenhouses and plant factories. Through that, resource optimization can be achieved. To predict the plant physiological processes and implement them in control actions of interest, a reliable monitoring system and a capable control system are needed. In this paper, we focused on the option to use real-time crop monitoring for precision climate control in greenhouses. For that, we studied the processes and external factors influencing leaf net CO_2 assimilation rate (A_L, µmol CO_2 m^{-2} s^{-1}) as possible variables of a plant performance indicator. While measured greenhouse environmental variables such as light, temperature, or humidity showed a direct relation between A_L and light-quantum yield of photosystem II (Φ_2), we defined three objectives: (1) to explore the relationship between climate variables and A_L, as well as Φ_2; (2) create a simple and reliable method for real-time prediction of A_L with continuously Φ_2 measurements; and (3) calibrate parameters to predict chloroplast electron transport rate as input in A_L modelling. Due to practical obstacles in measuring CO_2 gas-exchange in commercial production, we explored a method to predict A_L by measuring Φ_2 of leaves in a commercial hydroponic greenhouse tomato crop ("Pureza"). We calculated A_L with two different approaches based on either the negative exponential response model with simplified biochemical equations (marked as Model I) or the non-rectangular hyperbola full biochemical photosynthetic models (marked as Model II). Using Model I can only be used to predict A_L with large uncertainty (R^2 0.64; RMSE 2.21), while using Φ_2 as input to Model II could be used to improve the prediction accuracy of A_L (R^2 0.71; RMSE 1.98). Our results suggests that (1) Φ_2 light signals can be used to predict net photosynthesis rate with high accuracy; (2) a parameterized photosynthetic electron transport rate model is suitable predicting measured electron transport rate (J) and A_L. The system can be used

as decision support system (DSS) for plant and crop performance monitoring when leaf-dynamics are up-scaled to the plant or crop level.

INTRODUCTION

In modern greenhouses and plant factories plant cultivation is usually done with computerized environmental climate control. To achieve the desired climate, a great variety of controllers and actuators are used (Körner and Van Straten, 2008; Rytter et al., 2012; Shamshiri et al., 2017; Gurban and Andreescu, 2018; Ramin et al., 2018), often supported by model-based decision support systems (DSS) (e.g. Körner, 2019). Although sensor-based monitoring and real-time model predictions strongly improved early warning and greenhouse climate control (Körner and Hansen, 2012; Mahlein, 2015; Körner, 2019), real-time crop monitoring still suffers from inadequate equipment and/or insufficiently model quality. The realization of soft-sensors (i.e. mathematical models using real-time sensor data) (De Koning, 2006) with deterministic explanatory models in greenhouse cultivation monitoring is still under development. In here, robust and simple sensors combined with models calibrated with data from laboratory experiments would be the most suitable approach to implement physiological based automatic control system in the greenhouse (Janka et al., 2013; Körner, 2019). To achieve that, a reliable system with both measured and modelled plant physiological parameters is needed.

Plant photosynthesis is a physiological process suitable to be used in DSS-development with monitoring and assessment tools. A monitoring system, initially based on measuring leaf net CO_2 exchange (A_L), was used as starting point in this study (BERMONIS, Steinbeis GmbH & Co. KG for Technology Transfer, Berlin, Germany). BERMONIS is real time photosynthesis monitoring system developed for long-time continuously measurement leaf gas exchange (Schmidt, 1998; Schmidt, 2005). The system can be used to up-scale multiple measured single leaf A_L to crop photosynthesis (A_{crop}, µmol CO_2 m^{-2} s^{-1}) by considering the variations of both light distribution and specific leaf photosynthetic capacity within the plants' canopy; e.g. Huber (2011) used BERMONIS in combination with psychrometric charts to detect and follow the "comfort zone" for an adult tomato crop in real-time.

Another widely used and accepted approach to measure plant photosynthetic productivity is chlorophyll fluorescence analysis (CFA). With the pulse amplitude modulation method of CFA (PAM), the light beams are modulated and the system detects fluorescence excited by the measuring light in the presence of background illumination (Schreiber, 1986; Schreiber et al., 1986; Govindjee, 1995; Schreiber, 2004; Baker, 2008; Tschiersch et al., 2017). Its small size, ease to transfer, and high sensitivity have made PAM-CFA a widely accepted method for plant stress detection (Lawlor, 1995; Cornic and Massacci, 1996; Flexas et al., 1998; Flexas et al., 2000; Lawlor and Cornic, 2002). In comparison to the gas exchange method used for plant photosynthetic productivity

measurements, CFA is more sensitive to plant water deficit: Water deficit leads to closed stomata that limits CO_2 uptake, followed by reduced energy use and excessive light energy absorption. This results in an activated protection mechanism and increase of non-photochemical quenching (NPQ), which is one of the main variables used in CFA. This process is commonly faster than gas exchange (Herppich et al., 1996; Herppich and Peckmann, 1997; Herppich and Peckmann, 2000). Therefore, it is of great practical significance to apply CFA parameters to simulate the CO_2 assimilation of plant leaves (Krall and Edwards, 1992; Edwards and Baker, 1993; Von Caemmerer, 2013). In addition, CFA can solve the problem of inconvenient operation of leaf gas-exchange measurement in production, for example, the installation of leaf chambers (e.g. BERMONIS) and the inspection of their air tightness (the main obstacles of leaf gas exchange in commercial greenhouse production). While both methods are suitable to measure plant photosynthetic productivity (each with pros and cons), the cuvette based leaf gas exchange measuring method delivers direct measurement response, while CFA is an indirect procedure but with a faster response in some situations.

With the underlying physiological process of plant photosynthesis, CFA provides insights into the relationship between chloroplast electron transport rates and carbon metabolism. Some scholars reported that CFA parameters could be used to indirect predict A_L by measuring the electron transport rateof PSII (J_f) as under some conditions a linear relationship between A_L and J_f exists (Krall and Edwards, 1992; Herppich and Peckmann, 2000; Yin and Struik, 2009). In addition, quantum yield of PSII (Φ_2) shows linear correlated with quantum yield of CO_2 fixation (Edwards and Baker, 1993). These results are often obtained under favorable experimental conditions, e.g. when light radiation (I, µmol m^{-2} s^{-1}) linearly increases during controlled light response curve measurements.

This study provides a valuable data set of photosynthetic physiological responses of plants in a dynamic production environment. Furthermore, it provides a method for estimating A_L by using the chlorophyll fluorescence parameters, and provides an approach for maximizing photosynthesis by manipulating the environmental conditions with real-time detection of limiting factors of leaf photosynthesis in greenhouse environments.

MATERIALS AND METHODS

Model Background

Around four decades ago a nowadays widely used biochemical photosynthesis model was proposed (Farquhar et al., 1980) (hereafter "FvCB model"). This model estimates A_L as

minimum of the Rubisco limited rate (A_c, μmol CO_2 m^{-2} s^{-1}), the electron (e$^-$) transport limited rate (A_j, μmol CO_2 m^{-2} s^{-1}), and the triose phosphate utilization limited rate (A_p, μmol CO_2 m^{-2} s^{-1}) of CO_2 assimilation (Eqn. 1). Abbreviations for parameters are defined in **Table 1**.

$$A_L = \min(A_c, A_j, A_p) \tag{1}$$

The value of Rubisco limited rate (A_c) is calculated as a function of the maximum carboxylation rate (V_{Cmax})

$$A_c = \frac{(C_c - \Gamma^*)\ V_{Cmax}}{C_c + K_{mC}(1 + O/K_{mO})} - R_d \tag{2}$$

where C_c is the CO_2 partial pressure at the carboxylation sites of Rubisco, K_{mC} and K_{mO} are Michaelis-Menten constants of Rubisco for CO_2 and O_2, respectively (Farquhar et al., 1980). R_d is the mitochondrial respiration of leaves.

According to the usage of energy suppliers NADPH and ATP, two similar equations with different parameter values (Eqns. 3 and 4) were used to estimate the RuBP-regeneration limitation, which is a function of the electron (e$^-$) transport J:

$$A_j = \frac{(C_C - \Gamma_*)J}{4C_C + 8\Gamma^*} - R_d \tag{3}$$

$$A_j = \frac{(C_C - \Gamma_*)J}{4.5C_C + 10.5\Gamma^*} - R_d \tag{4}$$

Theoretically, J can be assessed by CFA (then J becomes J_f). J_f is given by:

$$J_f = I_{inc} \cdot abs \cdot \rho_2 \cdot \Phi_2 \tag{5}$$

where abs is the proportion of incident light that is absorbed by the leaf. It is frequently assumed to be 0.84 (Maxwell and Johnson, 2000) or 0.85 (Von Caemmerer, 2000); ρ_2, is the fraction of absorbed light transported to PSII (frequently assumed to be 0.48; Von Caemmerer, 2000).

J_f is assumed equal to the rate of e$^-$ transport through PSII (J_2), while J_2 is the rate of e$^-$ transport through PSI. The rate of cyclic e$^-$ transport J_{cyc} is $f_{cyc} \cdot J_1$, where f_{cyc} is a fraction of e$^-$ follows the cyclic path (see **Figure 1**). This leads to the following balance as proposed by Yin et al. (2004).

$$J_2 + f_{cyc} \cdot J_1 = J_1 \tag{5-1}$$

We define all electron transport through PSI reaction center as 1, as well as the fractions e- for the cyclic and pseudocyclic paths (f_{cyc} or f_{pseudo}, respectively). The remaining fraction ($1 - f_{cyc} - f_{psedo}$) is transferred to NADP$^+$. The electron transport for NADP$^+$ reduction (J_{NADP^+}) can thus be formulated as:

$$J_{NADP^+} = \left(1 - f_{cyc} - f_{pseudo}\right) \cdot J_1 \tag{5-2}$$

Combining Eqn. (5-1) and Eqn. (5-2), Eqn. (5-3) can be derived.

$$J_{NADP^+} = \left(1 - f_{cyc} - f_{pseudo}\right) \cdot \frac{J_2}{(1 - f_{cyc})} \tag{5-3}$$

We assume the environment is steady state, the pseudocyclic path, which may occur at high light condition to produce oxygen
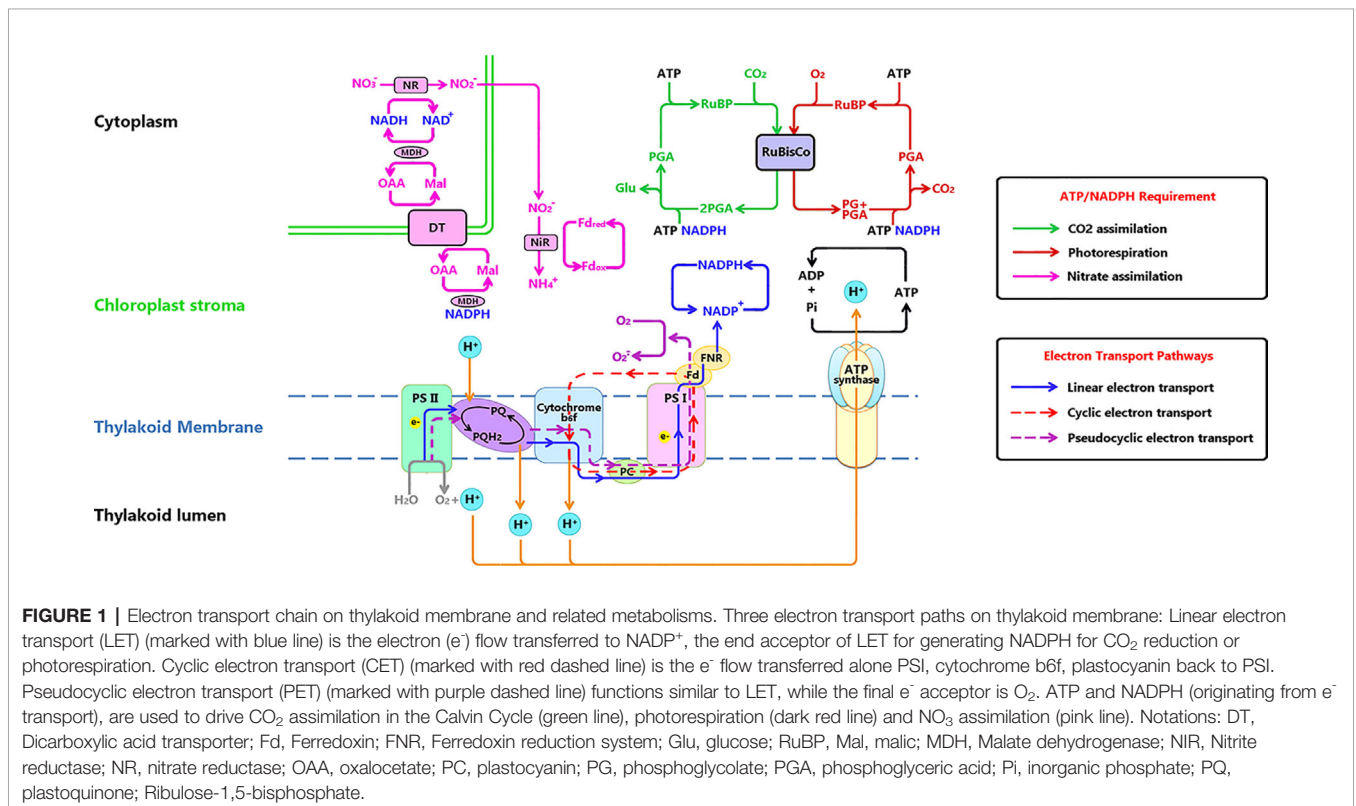

FIGURE 1 | Electron transport chain on thylakoid membrane and related metabolisms. Three electron transport paths on thylakoid membrane: Linear electron transport (LET) (marked with blue line) is the electron (e$^-$) flow transferred to NADP$^+$, the end acceptor of LET for generating NADPH for CO_2 reduction or photorespiration. Cyclic electron transport (CET) (marked with red dashed line) is the e$^-$ flow transferred alone PSI, cytochrome b6f, plastocyanin back to PSI. Pseudocyclic electron transport (PET) (marked with purple dashed line) functions similar to LET, while the final e$^-$ acceptor is O_2. ATP and NADPH (originating from e$^-$ transport), are used to drive CO_2 assimilation in the Calvin Cycle (green line), photorespiration (dark red line) and NO_3 assimilation (pink line). Notations: DT, Dicarboxylic acid transporter; Fd, Ferredoxin; FNR, Ferredoxin reduction system; Glu, glucose; RuBP, Mal, malic; MDH, Malate dehydrogenase; NIR, Nitrite reductase; NR, nitrate reductase; OAA, oxalocetate; PC, plastocyanin; PG, phosphoglycolate; PGA, phosphoglyceric acid; Pi, inorganic phosphate; PQ, plastoquinone; Ribulose-1,5-bisphosphate.

radicals O_2^- () is not considered, in this study ($f_{pseudo} = 0$), means that:

$$J_{NADP^+} = J_2 = J_f \qquad (5 - 4)$$

Finally, at high CO_2 partial pressure (particularly in combination with high radiation) the rate of A_L is sometimes limited by the release of inorganic phosphate (P_i). Starch and sucrose synthesis may become inadequate to recycle the P_i sequestered in the production of triose phosphates, in which case P_i may become limiting (Woodrow and Berry, 1988; Harley and Sharkey, 1991; Lombardozzi et al., 2018). The P_i limited part of A_L (A_p) is calculated as:

$$A_p = \frac{3 \ T_p(C_C - \Gamma_\star)}{C_C - (1 + 3\alpha_g)\Gamma^\star} - R_d \qquad (6)$$

Where T_p is the triose-phosphate use (TPU) rate and α_g is the non-returned fraction of glycolate.

In Eqns. 2 to 4 and Eqn. 6, the CO_2 concentration on the chloroplast side (C_c, μmol mol^{-1}) is calculated from the pathway of ambient CO_2 (C_a, μmol mol^{-1}) through leaf surface (C_s, μmol mol^{-1}) and intercellular air spaces (C_i, μmol mol^{-1}) to the chloroplast (Flexas et al., 2008; Flexas et al., 2012).

The leaf conductances to CO_2, i.e. boundary layer conductance (g_b, mmol CO_2 m^{-2} s^{-1}), stomatal conductance (g_s, mmol CO_2 m^{-2} s^{-1}) and mesophyll conductance (g_m, mmol CO_2 m^{-2} s^{-1}) are factors influencing C_c. (Yin et al., 2009a) Due to the complicated leaf gas-exchange measurements for g_m estimation, intercellular CO_2 concentration is commonly assumed as: $C_i = C_c$ (Farquhar et al., 1980; Ethier and Livingston, 2004; Manter and Kerrigan, 2004; Sun et al., 2014). However, as g_m is a major variable in photosynthesis, neglecting g_m will result in inaccurate prediction of A_L (Nobel, 1977; Nobel, 1983; Warren, 2006; Pons et al., 2009; Yin and Struik, 2009; Yin et al., 2009a; Yin and Struik, 2012). The influence of this potential error in prediction A_L has been considered and discussed in this study.

Two equations (Eqns. 3 and 4) were used to simulate electron transport limitation. The detailed derivation process is well described by Von Caemmerer (2000) and Yin et al. (2004). To simplify, in the production of NADPH and ATP, electron transport and the concomitant proton transfer in the chloroplast thylakoids are central processes. Carboxylation and oxygenation in C_3 metabolic reactions requires NADPH and ATP. Farquhar proposed that each carboxylation requires 2 NADPH and 3 ATP, and each oxygenation requires 2 NADPH and 3.5 ATP. In Eqn. 3, the regeneration of RuBP is assumed restricted by NADPH, the rate of whole chain electron transport required to support NADPH consumption by the photosynthetic carbon reduction (PCR) and photorespiratory carbon oxidation (PCO) cycles during CO_2 fixation (Von Caemmerer and Farquhar, 1981; Dubois et al., 2007; Sharkey et al., 2007). Therefore, oxygenation to carboxylation ratio is given by 2 Γ^*/C_i (Farquhar and von Caemmerer, 1982). The rate of NADPH consumption can be expressed as $(2 + 4\Gamma^*/C_i)V_c$, where V_c is the rate of carboxylation. Since the reduction of one NADP$^+$ to NADPH requires two e$^-$, the rate of e$^-$ transport for satisfying the NADPH requirement is $(4 + 8\Gamma^*/C_i) V_c$ (**Figure 2**).

In Eqn. 4, the regeneration of RuBP is not only limited by NADPH, but also by ATP (Von Caemmerer and Farquhar, 1981; Bernacchi et al., 2003; Long and Bernacchi, 2003; Yin and Struik, 2009). The rate of ATP consumption in C_3 reaction is $(3 + 7\Gamma^*/C_i) V_c$. The FvCB model assumes that 3 H$^+$ are required for the photophosphorylation of 1 ADP to 1 ATP. Therefore, the flow of one e$^-$ via the linear chain produces 2/3 ATP. Assuming ATP is produced by the linear e$^-$ transport alone, the required rate of the linear e$^-$ flow is $(4.5 + 10.5\Gamma^*/C_i) V_c$ (**Figure 2**) (Yin et al., 2004).

One key point of this study is the use of CFA to predict A_L. Foyer and Noctor, 2002 Since the Mehler reaction (Mehler, 1951) is not subject to this study, we solely use the linear electron transport of steady state photosynthesis in Eqns. 3 and 4. ATP and NADPH are used to drive the CO_2 assimilation, photorespiration and NO_3^- assimilation (see **Figure 1**) (Robinson, 1987; Noctor and
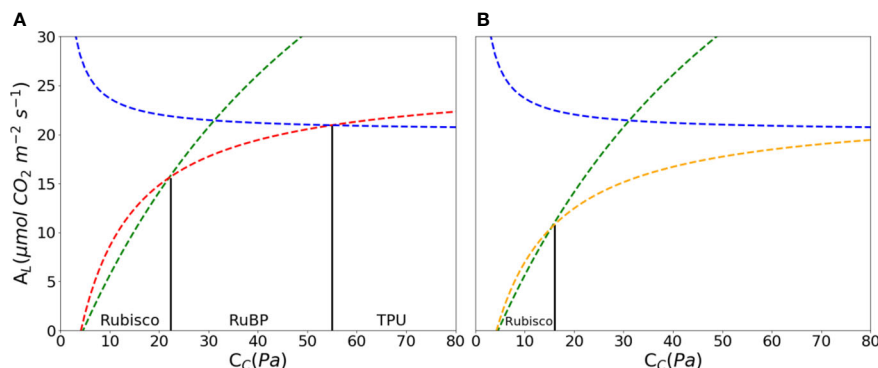

FIGURE 2 | CO_2 assimilation **(A)** as a function of chloroplast partial pressure of CO_2 (C_C) according to the FvCB model. With increasing Cc, A_L is limited by ribulose-1, 5-bisphosphate (RuBP) carboxylase/oxygenase (Rubisco) marked with green, RuBP marked with red in A and orange in B; triose-phosphate utilization (TPU) marked with blue, respectively. Rubisco kinetics parameters were using values of **Table 1** in Sharkey et al. (2007): K_C = 27.24 Pa, K_O = 16.58 kPa, O = 21 kPa, Γ^* = 3.74 Pa. Other parameters: R_d = 1.0 μmol·m–2·s–1, V_{Cmax} = 97.0 μmol·m–2·s–1, J_{max} = 144.0 μmol·m^{-2}·s^{-1}, T_p = 7.1 μmol·m^{-2}·s^{-1}, α_g = 0.15 μmol CO_2 m^{-2}s^{-1}. Abbreviations for parameters are defined in **Table 1**. The RuBP limitation is calculated with Eqn. 3 **(A)** and Eqn. 4 **(B)**.

TABLE 1 | Abbreviation used in this study.

Abb.	Definition	Unit
A_L	Net photosynthesis rate	$\mu mol\ CO_2\ m^{-2}s^{-1}$
A_c	Rubisco activity limited net photosynthesis rate	$\mu mol\ CO_2\ m^{-2}s^{-1}$
A_{gl}	Gross leaf assimilation rate	$\mu mol\ CO_2\ m^{-2}s^{-1}$
A_{glmax}	Maximum gross assimilation rate	$\mu mol\ CO_2\ m^{-2}s^{-1}$
A_j	Electron transport limited net photosynthesis rate	$\mu mol\ CO_2\ m^{-2}s^{-1}$
A_P	Triose phosphate utilization limited net photosynthesis rate	$\mu mol\ CO_2\ m^{-2}s^{-1}$
C_a	Ambient air CO_2 partial pressure or concentration	μbar
C_c	Chloroplast CO_2 partial pressure	μbar
C_i	Intercellular CO_2 partial pressure	μbar
F	Leaf chlorophyll fluorescence yield of light acclimated state	–
Fm'	maximal fluorescence yield of the light acclimated state	–
f_{OC}	Ration of maximum oxygenation rate to maximum carboxylation rate	–
f_{cyc}	A fraction of e- follows the cyclic mode around PS I	–
f_{pseudo}	A fraction of e- follows the pseudocyclic mode for O_2 reduction.	–
g_b	Boundary layer conductance	$mol\ m^{-2}s^{-1}$
g_m	Mesophyll diffusion conductance	$mol\ m^{-2}s^{-1}$
g_s	Stomatal conductance	$mol\ m^{-2}s^{-1}$
I	Solar radiation	$\mu mol\ [photon]\ m^{-2}s^{-1}$
I_{abs}	Photon flux density absorbed by leaf photosynthetic pigments	$\mu mol\ [photon]\ m^{-2}s^{-1}$
I_{inc}	Photon flux density incident to leaves	$\mu mol\ [photon]\ m^{-2}s^{-1}$
J_1	e- transport rate through PSI	$\mu mol\ [e^-]\ m^{-2}s^{-1}$
J_2	e- transport rate through PSI	$\mu mol\ [e^-]\ m^{-2}s^{-1}$
J_f	Rate of e- transport calculated from the chlorophyll fluorescence measurement	$\mu mol\ [e^-]\ m^{-2}s^{-1}$
J_{NADP+}	The electron transport for the NADP+ reduction	$\mu mol\ [e^-]\ m^{-2}s^{-1}$
J_{max}	Maximum value of J under saturated light	$\mu mol\ [e^-]\ m^{-2}s^{-1}$
K_C	Michaelis–Menten constant of Rubisco for CO_2	μbar
K_O	KmO Michaelis–Menten constant of Rubisco for O_2	$mbar$
M_{CO2}	Molar mass of CO_2	$kg\ mol^{-1}$
O	Oxygen partial pressure	$mbar$
P	Pressure	Pa
PAR	Photosynthetically active radiation	$\mu mol\ m^{-2}s^{-1}$
P_i	inorganic phosphate	
R	Gas constant	$J\ kg^{-1}\ K$
r_{b_co2}	Boundary layer resistance to CO_2 diffusion	$s\ m^{-1}$
r_{C_co2}	Carboxylation resistance to CO_2 diffusion	$s\ m^{-1}$
r_{s_co2}	Stomatal resistance to CO_2 diffusion	$s\ m^{-1}$
R_d	Day respiration (respiratory CO_2 release other than by photorespiration)	$\mu mol\ [CO_2]\ m^{-2}s^{-1}$
T_a	Air temperature	K
T_l	Leaf temperature	K
V_{Cmax}	Maximum rate of Rubisco activity-limited carboxylation	$\mu mol\ [CO_2]\ m^{-2}s^{-1}$
VPD	Vapour-pressure deficit between leaf and air	kPa
Γ^*	Cc-based CO_2 compensation point in the absence of Rd	μbar
θ_J	Factor for the degree of curvature	–
ρ_2	Proportion of Iabs partitioned to PSII	–
$\alpha_{(LL)}$	Initial quantum yield	$mol\ [e^-]\ (mol\ photon)$
α_g	Nonreturned fraction of glycolate	$\mu mol\ CO_2\ m^{-2}s^{-1}$
ϵ	Light use efficiency by photorespiration	$mg\ CO_2 J^{-1}$
Φ_2	Quantum efficiency of PSII e- flow on PSII-absorbed light basis, usually assessed from the chlorophyll fluorescence measurements	–

Foyer, 1998; Foyer and Noctor, 2002; Allen, 2003). In that, the assimilation of NO_3^- has a lower requirement of ATP/NADPH, and furthermore, the reducing power for NO_3^- assimilation may not directly originate from the chloroplast (Miflin, 1974; Yin et al., 2006; Walker et al., 2014). Meanwhile, whether the reductants and energy is come from linear electron transport is still unclear. The ferredoxin, NADPH, and ATP may partly be produced by cyclic or pseudocyclic electron flow. And the fraction for nitrate reduction is not a constant. It may depend on species, nutrient supply and growth stage (Yin et al., 2006). Due to the difficult endeavor of quantifying the proportion of electron flow for nitrate reduction in real time and the small proportion of it, the electron flow for NO_3^- assimilation was not considered in this study.

Plant Material, Growth Conditions

One hundred and forty-four tomato plants (cv. "Pureza") were cultivated in February 2016 in a 62.6 m² Venlo-type greenhouse at a commercial grower in Abtshagen, Germany (52°31'12.025" N; 13°24'17.834" E). The greenhouse had a side wall height of 4.2 m, equipped with double glass and single glass in the roof. The internal construction consisted of two double gutters in the middle and two single gutters beside the walls. Plants were planted in rock wools slabs with a common drip irrigation system. Seed was placed on rock-wall cubes on January 23rd 2016 and young plants were placed on the rock wools slabs two weeks after. Three weeks after transplanting, the measurements started. Temperature and humidity were controlled with pipe heating and passive roof ventilation. Set points for heating system were defined as 22 and 18°C for day and night, respectively; ventilation set point was 21°C day and night between April and October and 26°C for the rest of the year. The energy screen was unfolded one hour before sunrise and folded one hour after sunset. Between 7 a.m. and 8 p.m. supplementary light (high-pressure sodium lamps, HPSL) started when global radiations outside the greenhouse was below 20 W m⁻². Water and nutrients were adequately supplied to the needs of the crop. Nutrient solution was adjusted with mineral fertilizer to an electric conductivity (EC) of 1.8 dS m⁻¹ and a pH of 6.5. The nutrient concentration was used according to Lattauschke (2004) (**Table 2**).

Environment and Plant Photosynthesis Monitoring

The environmental variables air temperature, relative humidity, light, and CO_2 concentration (T_a, RH, I, and [CO_2], respectively) were recorded by a commercial greenhouse monitoring system (Growwatch, Fytagoras BV, Leiden, The Netherlands). In this system, plant photosynthetic active radiation (PAR) was measured (Li-190R, LICOR, Lincoln, Nebraska, USA) as photosynthetically photon flux density (PPFD, μmol m⁻² s⁻¹). The monitoring system was placed on an uncovered area (right next to the plant) at the height of the seventh unfolded leaf (calculated from the top, the fifth leaf was usually the first mature leaf). T_a and RH were measured by a commercial sensor for

TABLE 2 | Nutrient concentration for greenhouse tomato used in this study.

Nutrient	Abr.	Amount	Unit	Nutrient	Abr.	Amount	Unit
Nitrogen	N	151	mg L^{-1}	Iron	Fe	2.0	mg L^{-1}
Phosphorus	P	37	mg L^{-1}	Boron	B	0.3	mg L^{-1}
Potassium	K	234	mg L^{-1}	Copper	Cu	0.2	mg L^{-1}
Calcium	Ca	128	mg L^{-1}	Manganese	Mn	1.2	mg L^{-1}
Magnesium	Mg	24	mg L^{-1}	Molybdenum	Mo	0.05	μg L^{-1}
Sulphur	S	110	mg L^{-1}	Zinc	Zn	0.4	mg L^{-1}

volume applications (HMP60, VAISALA, Helsinki, Finland). Leaf temperature (T_l) of each seventh leaf of four plants was measured with an infrared radiation thermometer (CT11, HEITRONICS Infrarot Messtechnik, Wiesbaden, Germany). All variables were continuously measured and averaged over 5 min and stored on a central server. Outliers were detected according to Tukey (1977), i.e. an outlier is defined as a value that is smaller than the lower quartile minus 3 times the interquartile range, or larger than the upper quartile plus 3 times the interquartile range. Outliers and invalid measurements due to sensor calibration or failure were removed from the original data-set (Grubbs, 1950; Aggarwal and Yu, 2005). Scattered data outliers within PAR measurements as artifact based on sudden shade incidences hitting the PAR point-sensors during direct sunlight conditions (due to shade-spots of the greenhouse construction) were filtered with Savitzky-Golay filter (with order=3, window=21) (Orfanidis, 2006; Miranda, 2017); i.e., a mathematical procedure for smoothing data in order to increase data precision.

Leaf CO_2 gas-exchange (GE) was recorded by the BERMONIS system, measuring the lump-sum of CO_2 gas exchange of eight leaves and calculated to an averaged A_L. Likewise, measurements of T_l, the eight cuvettes were set at each seventh leaf of four plants. On each plant two opposing leaflets were used resulting in two cuvettes per plant. The fully expanded leaves were placed into the cuvettes (acting as transparent leaf chambers) with the leaves face-up, the metal frame supported the cuvettes in a horizontal position. A pilot experiment demonstrated the functionality of BERMONIS to commercial instruments (**Supplementary Material A**).

Leaf chlorophyll fluorescence yield of light acclimated state (F, -), and maximal fluorescence yield of the light acclimated state (F_m', -) were measured with a PAM monitor (Monitoring PAM, Walz, Effeltrich, Germany). The sensor was likewise BERMONIS set on the seventh leaves (on different plants). For that, F and F_m' were measured in the same time and quantum efficiency of PSII e$^-$ flow on Φ_2 of the leaf was calculated (Krause and Weis, 1984):

$$\Phi_2 = \frac{F_m' - F}{F_m'} \qquad (7)$$

The sensors were re-placed to new leaves after two weeks. Recorded data are shown in **Supplementary Material B**.

Model Development

A complete data set with environmental variables (T_a, T_l, RH, I, and [CO_2]), mean A_L, and Φ_2 was established for model validation and parameters calibration in this study and structured as shown in **Figure 3**. Four models were compared in this study: Model I, Model II$_a$ and Model II$_b$, and Model II$_b$* used in greenhouse leaf photosynthesis modelling (**Table 3**).
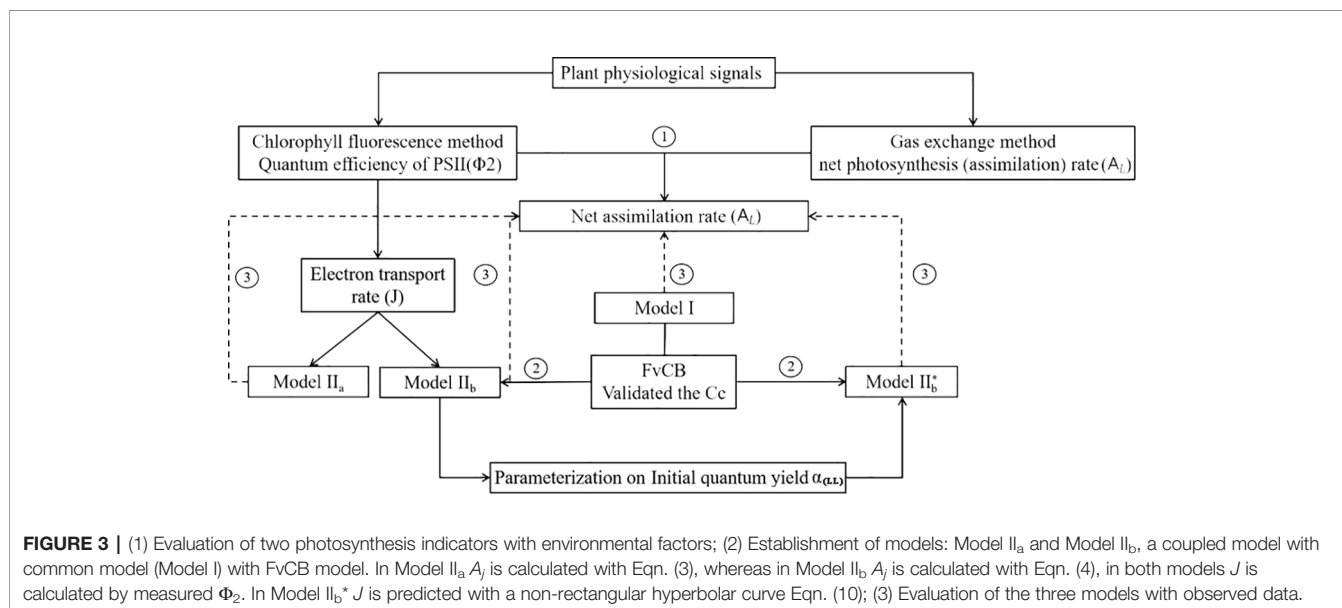

FIGURE 3 | (1) Evaluation of two photosynthesis indicators with environmental factors; (2) Establishment of models: Model II$_a$ and Model II$_b$, a coupled model with common model (Model I) with FvCB model. In Model II$_a$ A_j is calculated with Eqn. (3), whereas in Model II$_b$ A_j is calculated with Eqn. (4), in both models J is calculated by measured Φ_2. In Model II$_b$* J is predicted with a non-rectangular hyperbolar curve Eqn. (10); (3) Evaluation of the three models with observed data.

TABLE 3 | A summary of model formulas.

Model	Calculation equations
Model I	Eqn. (8), (9) & **Supplementary Material C**
Model II$_a$	Use Model I and Eqn.(11),(12) to calculate C_C, Eqn.(5) to simulate J, Eqn.(1),(2),(3),(6) to simulate A_L
Model II$_b$	Use Model I and Eqn. (11),(12) to calculate C_C, Eqn.(5) to simulate J, Eqn.(1),(2),(4),(6) to simulate A_L
Model II$_b$*	Use Model I and Eqn. (11),(12) to calculate C_C, Eqn.(10) to calculate J, Eqn.(1),(2),(4),(6) to simulate A_L

Model I is the negative exponential light response commonly used in greenhouse leaf photosynthesis modelling (Thornley, 1976; Gijzen, 1992; Goudriaan and Van Laar, 1994; Körner et al., 2002; Körner, 2004). Model II$_a$ and II$_b$ use Model I as basis and further employ the complete FvCB model with two different equation to estimate Aj. In these models, J is estimated by detected Φ_2 (Eqn. 5). In Model II$_b$*, J is calculated with the non-rectangular hyperbolar curve (Eqn. 10).

Model I

In Model I, A_L is determined from gross leaf assimilation rate (A_{gl}, μmol CO_2 m^{-2} s^{-1}) minus leaf day respiration (R_d, μmol CO_2 m^{-2} s^{-1}).

$$A_L = A_{gl} - R_d \quad (8)$$

A_{gl} is determined from light use efficiency ϵ and maximum gross assimilation rate A_{glmax} with the negative exponential light-response curve (Goudriaan and Van Laar, 1994) using absorbed radiation (I_{abs}) as input.

$$A_{gl} = A_{glmax} \cdot \left(1 - e^{-\frac{\epsilon \, I_{abs}}{A_{glmax}}}\right) \quad (9)$$

This leaf photosynthesis light response model is commonly used to upscale leaf photosynthesis to the crop level (A_{crop}) considering light distribution with Gaussian integration over the crop depth (Goudriaan and Van Laar, 1994). It is commonly used as basic photosynthesis model in many crop growth models for yield estimation (Spitters et al., 1989; Hoogenboom et al., 1990; Jones et al., 1991; Heuvelink, 1996). The description of the biochemical processes is simplified. The key parameters in this model could be identified by curve fitting or converted from V_{Cmax} or J_{max}. Detailed equations are shown in **Supplementary Material C**.

Model II$_a$/II$_b$

The steady-state version of the FvCB model has had the strongest impact and has become the standard model for photosynthesis of C_3 species (Sharkey, 1984; Sharkey, 1985; Farquhar et al., 2001; Long and Bernacchi, 2003). The models predicts photosynthesis as the minimum of the A_c, A_j, A_p (Eqn. 1, see Section Model background). In both Models II$_a$ and II$_b$, J is assessed by chlorophyll fluorescence J_f. While Model II$_a$ includes Eqn. 3, Model II$_b$ is using Eqn. 4 for A_j simulation.

Model II$_b$*

In Model II$_b$*, J is calculated with a non-rectangular hyperbolic curve of incident light (Farquhar and Wong, 1984). Solely

environmental variables were used for parameter fitting of Model II$_b$*.

$$J = \frac{J_{max} + \alpha_{(LL)} \cdot I_{abs} - \sqrt{\left(J_{max} + \alpha_{(LL)} \cdot I_{abs}\right)^2 - 4\theta_J \cdot J_{max} \cdot \alpha_{(LL)} \cdot I_{abs}}}{2\theta_J} \quad (10)$$

where I_{abs} μmol [photon] m^{-2}s^{-1} is the absorbed light; $\alpha_{(LL)}$ is a factor covert absorbed light to the useful light absorbed by PSII. Therefore, $\alpha_{(LL)} \cdot I_{abs}$ represents light absorbed by PSII. θ_J is a factor for the degree of curvature, assumed as 0.85 (Ögren and Evans, 1993; Von Caemmerer, 2000; Ethier et al., 2006).

Estimating Chloroplast CO_2 Partial Pressure

C_C is derived from the pathway of CO_2 from ambient C_a through leaf surface C_s and intercellular air spaces (C_i). Here, g_b, g_s and g_m are indicated (Flexas et al., 2008). We analyzed the predicted results with and without calculated g_m. According to Fick's first law of diffusion for CO_2 transfer along the path from C_a to C_c is given by:

$$C_C = C_i - A_L \left(\frac{1}{g_m}\right) \quad (11)$$

$$C_i = C_a - A_L \left(\frac{1}{g_b} + \frac{1}{g_s}\right) \quad (12)$$

As shown in Eqns. 11 and 12, A_L is required to be known a priori. To avoid infinite circulation of variables, the initial estimated A_L rate of Model I is used as starting point for C_c and C_i calculation.

In some calculations, C_i is treated equal to C_c (Leuning, 2010) and it was suggested setting g_m to be finite large ($g_m \to \infty$) (Björkman, 1973; Laisk et al., 2005). Then Eqn. 11 can be re-formulated to Eqn. 12 and thus the need for g_m will be redundant:

$$C_C \cong C_i = C_a - A \left(\frac{1}{g_b} + \frac{1}{g_s}\right) \quad (13)$$

We propose the Jarvis model as sub-model for g_b and g_s.

$$g_b = \frac{P}{R \cdot T \cdot r_{b\_co2}} \quad (14)$$

$$g_s = \frac{P}{R \cdot T \cdot r_{s\_co2}} \quad (15)$$

Where P/RT is the coefficient used to convert the resistance units (s m^{-1}) to molar units. r_{b_CO2} and r_{s_CO2} are the boundary-layer resistance and stomatal resistance respectively (**Supplementary Material C**).

Goudriaan and Van Laar (1994) suggested an equation for calculating carboxylation resistance (r_{C_CO2}). In theory, r_{C_CO2} can be used to calculate g_m as:

$$g_m = \frac{P}{R \cdot T \cdot r_{C\_co2}} \quad (16)$$

Consequently, the CO_2 partial pressure within the chloroplast was calculated with and without inclusion of g_m and the

respective results were compared. In this context C_C was calculated as:

1. Without g_m, assuming that $g_m \rightarrow \infty$; (See Eqn. 13)
2. With g_m based on the inverse r_{C_CO2}, namely $g_m = f(r_{C\_co2})$ (r_{C_co2} see **Supplementary Material C**)
3. With a hypothetical value, from the perspective of optimal fitting of the model, set g_m as 0.25 mol m^{-2} s^{-1}. This value (g_m = 0.25 mol m^{-2} s^{-1}) is consistent with an average mesophyll conductance of annuals herbaceous (Flexas et al., 2008; Yin et al., 2009b).

Estimating the Rate of Photosynthetic Electron Transport

The value of $\alpha_{(LL)}$ differs among published literature in e.g. Von Caemmerer, 2000; Niinemets et al. (2009), or Yin et al. (2009b). Three values of $\alpha_{(LL)}$ were compared: two values were reported in literatures (Niinemets et al., 2009; Yin et al., 2009b); one value was estimated with the parameter optimization method in this study ($\alpha_{(LL)}$ = 0.405).

Curve fitting was used for parameter estimation of g_m and $\alpha_{(LL)}$. The nonlinear least squares procedure available in python scipy.optimize tool box (function leastsq) was applied to minimize the sum of the residuals between measured data and predicted data (Madsen et al., 2004; Wallach et al., 2006; Salazar-Moreno et al., 2017).

Model-Parameterization

The biochemical parameters V_{Cmax} (µmol m^{-2} s^{-1}) and J_{max} (µmol m^{-2} s^{-1}) were assessed with an open leaf gas exchange measuring system (LI-6400, Li-Cor Inc., Lincoln, Nebraska, USA). The system was used to create CO_2-response curves (commonly referred to as A-Ci curve) at a CO_2 concentration set at a course of different set points (i.e. 400, 350, 300, 250, 200, 100, 400, 450, 500, 550, 600, 800, 1,000 µmol mol^{-1}), while keeping PAR at 1,500 µmol m^{-2} s^{-1} PPFD. Measurements were made at pre-set leaf temperature set points of 25°C and the system was set such that each CO_2 level was reached constant for several seconds and the measurement was recorded at this point. Data of the three measurements were averaged for further calculations. The A-Ci curve fitting was carried out using the Ethier and Livingston method (Ethier and Livingston, 2004; Ethier et al., 2006).

Statistical Analysis and Model Performance

For all statistical analyses, the statistical software package SPSS was used (version 23.0, UNICOM Global, CA, USA). Multiple linear regression (MLR) was used for examining A and Φ_2 response to multi-environmental variables: air temperature (T_a, K), vapour pressure deficit (VPD, kPa) and PAR. The coefficient of determination (R^2), root mean squared error (RMSE), and mean absolute error (MAE) were used to analyze the goodness-of-fit between the simulated value and the measured value. RMSE and MAE were used to evaluate the model performance. The smaller the RMSE and MAE value, the better the consistency between the

simulated and the measured value, thus the more accurate and reliable the model prediction becomes (Chai and Draxler, 2014).

RESULTS

Evaluation of Physiological Signals

Photosynthetic signals are indicators of plant health and can be used as variables to formulate control strategies, when compared with the expected optimum at current environmental conditions. For multi linear regression, the collinearity of factors needs to be taken into account. These environmental factors meet the collinearity diagnostics with the variance inflation factor less than 10 (data not shown). The resulting regression equations are presented in **Table 4**. The results showed that the environmental variables can better explain the variation of A_L than the variation in Φ_2: 61.5% of the variation of A_L could be assessed by T_a, VPD, and I, whereas only 50.2% of Φ_2 variation can be assessed by environmental factors Thus, in our measurements A_L is a better suited to evaluate plant responses to the environmental factors than Φ_2.

Model Validation and Parameters Calibration

In the present study, the method proposed by Ethier and Livingston (2004) was used to identify the biochemical parameters V_{Cmax}, J_{max}, R_d. With a well-fitting result (R^2 = 0.99; **Figure 4**). V_{Cmax25} = 71.0 µmol m^{-2} s^{-1}, J_{max25} =147.7 µmol m^{-2} s^{-1}, and R_{d25} = -0.34 µmol m^{-2} s^{-1} were used in the further modelling framework.

TABLE 4 | Multiple linear regression: the environmental variables explain variance in A_L and Φ_2.

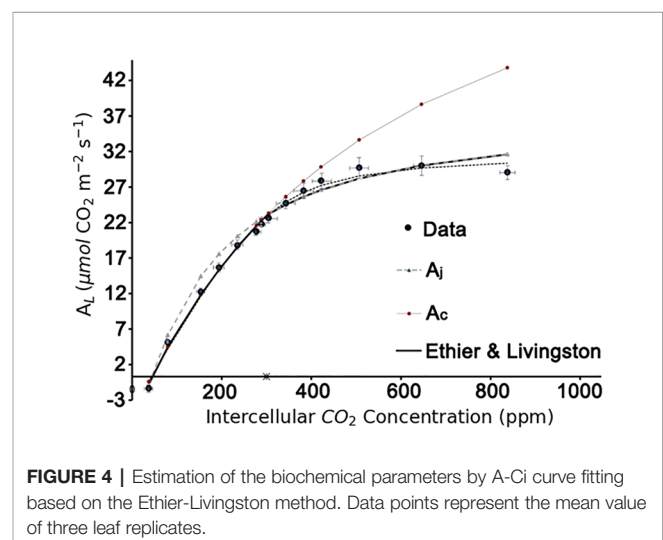| Ind.	Ta	VPD	PAR	Regression equation	R^2
A_L	69.73	11.01	19.26	y=-12.7+0.89Ta-1.43 VPD +0.002 PAR	0.615
Φ_2	79.90	17.18	3.34	y=1.1-0.02Ta+0.04 VPD +6.168×10-6 PAR	0.502

FIGURE 4 | Estimation of the biochemical parameters by A-Ci curve fitting based on the Ethier-Livingston method. Data points represent the mean value of three leaf replicates.
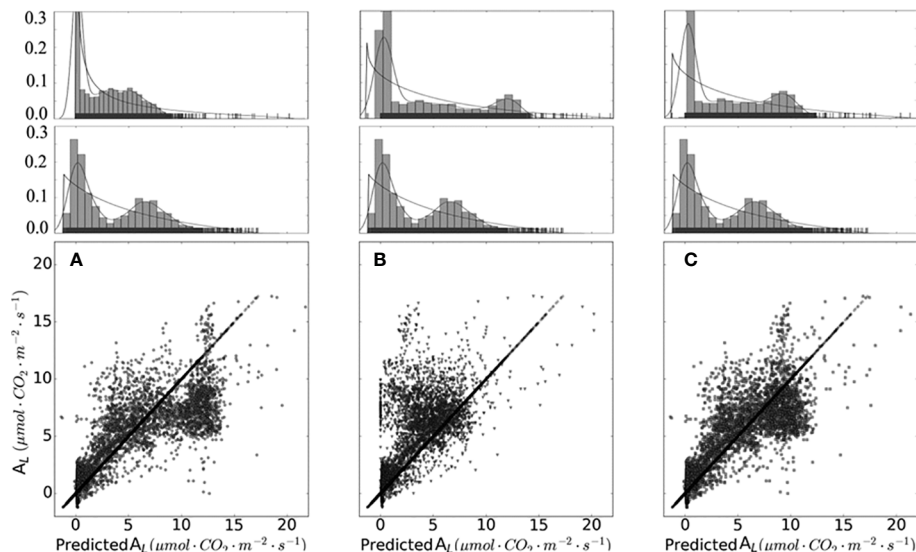
FIGURE 5 | Measured and simulated net photosynthesis rate based on different chloroplast CO_2 partial pressure. Data points shown in **(A)** were calculated with infinity mesophyll conductance (g_m). Data points shown in **(B)** were calculated based on converted r_{C_co2}. Data points shown in **(C)** were calculated with calibrated g_m equal to 0.25. On the top of **(A–C)** are sub-graphs, displaying the data distribution of each plot, on the middle layer of **(A–C)** displayed the distribution of measured data.

TABLE 5 | Coefficient of determination (R^2), root mean square of error (RMSE) and mean absolute error (MAE) of the linear regression calculated between the observations and simulations of mesophyll conductance g_m.

No.	g_m	R2	RMSE	MAE
1	$g_m \rightarrow \infty$	0.57	2.39	1.61
2	$g_m = f(r_C)$	0.52	2.56	1.61
3	$g_m = 0.25$	0.71	1.99	1.34

From **Figure 5** and **Table 5**, it is evident that calibrated g_m improved the prediction quality with the highest coefficient of determination (R^2), and achieved the lowest RMSE. Considering g_m infinite, the simulation results are overestimated. g_m, based on optimal fitting, equal to 0.25, achieved the highest R^2 and the lowest RMSE and MAE.

Eqns. 3 and 4 are two approaches to calculate A_j (**Table 7**). In Model II_b (using Eqn. 4) yielded a higher R^2 and lower RMSE compared to calculations with Model II_a (i.e. using Eqn. 3). Using Eqn. 10 to simulate the measured J_f, $\alpha_{(LL)}$ value impacted the prediction performance of the model. Three $\alpha_{(LL)}$ values were used in this study. From **Figure 6**, the results show that the calibrated parameters can largely improve the prediction quality (**Table 6**). RMSE and MAE decreased after applied the calibrated $\alpha_{(LL)}$ value, which indicated that the R^2 and RMSE between predicted value and measured value decreases after changing $\alpha_{(LL)}$ and was used for Model II_b*.

Model Test

The diurnal changes of the net photosynthesis rate and three models were illustrated in **Figure 7**. In contrast to Model I, the three versions of Model II (Model II_a, Model II_b and Model II_b*)

improved the prediction of A_L (i.e. higher R^2, **Table 7**). Implementing the predictions obtained from CFA into the model family Model II (i.e. with Model II_b) yielded in a high R^2 of 0.71. In addition, parameterization of $\alpha_{(LL)}$ as part of calculation of J (Eqn. 10) could be used to well predict A_L.
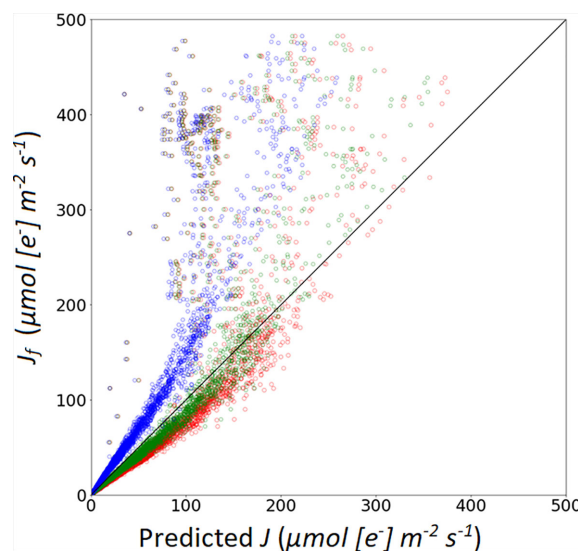

FIGURE 6 | Simulation of photosynthetic electron transport rate based on: A recommended value of α from Niinemets et al. (2009), marked with red open circles; a recommended α value from Yin et al. (2009b), marked with blue open circles; a calibrated α value (0.405), marked with green open circles.

TABLE 6 | Coefficient of determination (R^2), root mean square of error (RMSE) and mean absolute error (MAE) of the linear regression calculated between the observations and simulations of electron transport rate J calculated with the three conversion factors ($\alpha_{(LL)}$) values.

Marked color	$\alpha_{(LL)}$ value	reference	R^2	RMSE	MAE
blue	0.24	Yin et al., 2009b	0.85	52.76	18.4
green	0.40	Optimized	0.74	47.35	13.58
red	0.46	Niinemets et al. (2009)	0.70	47.76	16.08

TABLE 7 | Coefficient of determination (R^2), root mean square of error (RMSE) of the linear regression calculated between the observations and Models.

Model	R^2	RMSE	MAE
Model I	0.64	2.21	1.50
Model II$_a$	0.70	1.99	1.34
Model II$_b$	0.71	1.98	1.33
Model II$_b$*	0.71	1.99	1.34

Model Application

During night, the ambient CO_2 concentration in the greenhouse increases due to plant respiration (**Figure 8**). At this time, the limiting factor of photosynthesis is the insufficient electron transfer efficiency of chloroplasts caused by insufficient light. During the light period, photosynthesis consumes ambient CO_2, and without CO_2-supply its concentration in the greenhouse air

rapidly decreases. Under this condition, the limiting factor of photosynthesis is shifted to "Rubisco-limitation", a close relation to ambient CO_2 concentration (**Figure 8**).

Based on our designed soft-sensor system, the CO_2 concentration required by plants in the current cultivation environment can be calculated accurately. For instance, as illustrated in **Figure 9** (before 01:00 p.m.), supplying excessive CO_2 to concentrations of 1,000 µmol mol^{-1} under insufficient lighting conditions does not improve the rate of photosynthesis, resulting in the waste of CO_2 (Schmidt, 1998). Meanwhile, when dosing extra CO_2, duo to the limited inorganic phosphate (P_i) TPU limitation is likely to occur. The soft-sensor can improve the understanding and control of plant photosynthesis, so as to potentially improve greenhouse climate control.

DISCUSSION

Net photosynthesis prediction in a tomato crop can be improved significant when on-line measurements with sensor systems and intelligent algorithms of models are combined to a so-called soft-sensor (De Koning, 2006; Körner, 2019). Here, the combination of real-time chlorophyll fluorescence measurements and photosynthesis models is suggested. However, when model-predicted rates of CO_2 exchange are compared with measured gas exchange, measuring accuracy of a gas exchange measurement system may complicate the determination of the
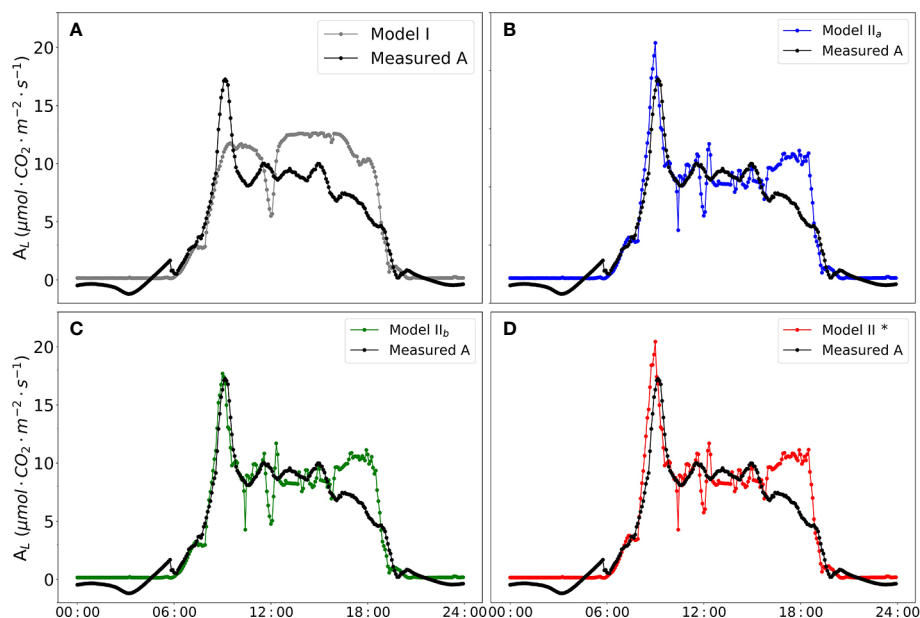

FIGURE 7 | Diurnal dynamics of net photosynthesis rate. Data points shown in black circles are actual value measured by BERMONIS **(A–D)**. Data points shown in filled gray circles in **(A)** are net photosynthesis rate calculated with Model I. Data points shown in filled blue circles in **(B)** are calculated with Model II$_a$. Data points shown in filled green circles in **(C)** are calculated with Model II$_b$. Data points shown in filled red circles in **(D)** are calculated with Model II$_b$*. V_{Cmax} = 71.0 µmol CO_2 m^{-2} s^{-1}, J_{max} = 147.7 µmol [e$^-$] m^{-2} s^{-1}, R_d = -0.34 µmol CO_2 m^{-2} s^{-1}, g_m = 0.25 mol m^{-2} s^{-1} were applied in the Model II$_a$, Model II$_b$ and Model II$_b$*. In Model II$_b$* $\alpha_{(LL)}$ =0.405 was applied in the modelling framework.
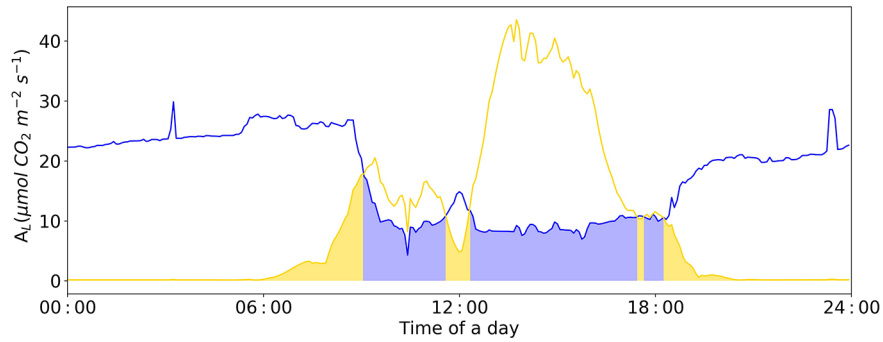
FIGURE 8 | Diurnal dynamics of net photosynthesis rate for Rubisco and electron-transport limited rates calculated with Model II$_b$. The Blue line represents Rubisco carboxylation-limited assimilation rate (A_c). The yellow line represents electron transport-limited assimilation rate (A_j). The yellow area represents leaf assimilation limited by A_j; the blue area represents leaf assimilation limited by A_c. V_{Cmax} = 71.0 μmol CO_2 m^{-2} s^{-1}, J_{max} = 147.7 μmol e$^-$ m^{-2} s^{-1}, R_d = -0.34 μmol CO_2 m^{-2} s^{-1}, g_m = 0.25 mol m^{-2} s^{-1} were applied in the Model II$_b$.
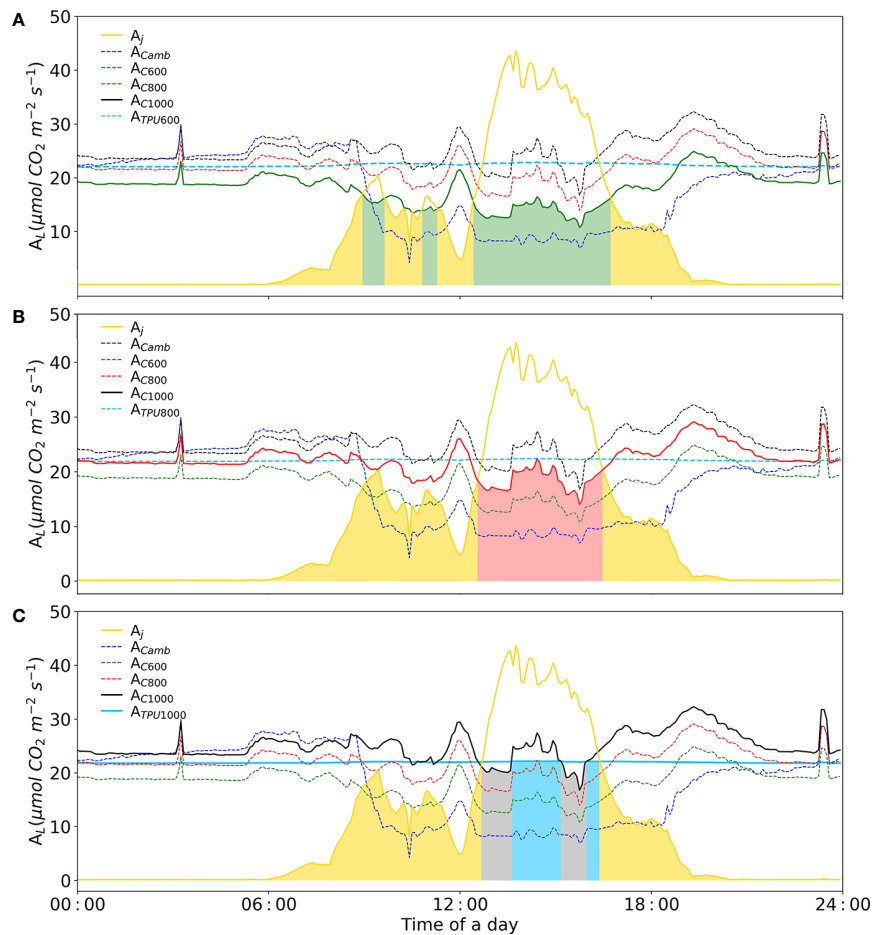

FIGURE 9 | Diurnal dynamics of net photosynthesis rate for electron-transport and carboxylation limited rates calculated with Model II$_b$. **(A)** Simulation of diurnal net photosynthesis rate with air CO_2 concentration of 600 μmol mol^{-1}. **(B)** Simulation of diurnal net photosynthesis rate with air CO_2 concentration of 800 μmol mol^{-1}. **(C)** Simulation of diurnal net photosynthesis rate with air CO_2 concentration of 1000 μmol mol^{-1}. The yellow line represents electron transport-limited assimilation rate (A_j). The blue dashed-line represents rubisco carboxylation-limited assimilation rate (A_c) at the given CO_2 concentration. The sky-blue line represents the TPU limited assimilation with corresponding CO_2 concentration. The three colors, green, red and black represent simulations with three CO_2 concentrations, i.e. 600, 800, 1000 μmol mol^{-1}, respectively. The colored area represents leaf assimilation rate. V_{Cmax} = 71.0 mmol CO_2 m^{-2} s^{-1}, J_{max} = 147.7 mmol e- m^{-2} s^{-1}, Rd = -0.34 mmol CO_2 m^{-2} s^{-1}, gm = 0.25 mol m^{-2} s^{-1} were applied.

true net photosynthesis. In this study, with the BERMONIS (Schmidt, 1998; Schmidt, 2005) a well-tested multi-leaf cuvette system was used for gas exchange measurements (Huber, 2011; Dannehl et al., 2014).

Another problem in designing soft-sensors often lies in the model structures. Here the difficulty is the unsuitability of the models for direct usage in a soft-sensor. The prediction efficiency of the used models depend among others on the identification and the estimation of substrate concentration, the chloroplast CO_2 partial pressure (C_C), and the photosynthetic electron transport rate (J). While (C_C) can be estimated from the calculated intercellular CO_2 concentration (C_i), A_L and g_m needs to be known beforehand. However, in general, C_i and A_L are also unknown at the beginning and a consequential model nesting tends to get trapped in infinite loop in simulations. Therefore, the key issue of using the FvCB models to calculating the actual photosynthetic rate is to accurately provide C_C and J data, either attained through model calculations or by measurements. To solve this problem, a commonly used but simplified biochemical A_L-model with negative exponential light-response (Model I) was coupled with the full biochemical model approach based on Farquhar et al. (1980) for calculating C_C, for which, in turn, g_m needed to be identified. Niinemets et al. (2009) and Flexas et al. (2012) evaluated the importance of g_m in estimation of net photosynthesis rate. It was demonstrated that a hypothetical situation, with $g_m \rightarrow \infty$, which means there is no diffusion restriction in the mesophyll, resulted in higher daily photosynthesis, than any other parameterization. This is consistent with the conclusion of this study. Due to the assumption of a finite g_m, a resistance between intercellular air spaces and the Rubisco carboxylation-sites in chloroplasts was used (Farquhar and Wong, 1984; Flexas et al., 2008). Results show that this equation does not fit A_L very well. However, at daytime, the lower g_m value resulted in lower C_C values and led to the underestimation of A_L. Therefore, we recommend a "universal" or cultivar dependent correction factor, or the usage of estimating g_m according to different experiments.

For A_L model estimations with Model I (used by Körner, 2004), maximum carboxylation rate and maximum electron transport rate (V_{Cmax} and J_{max}) need to be known. A general model for calculation of V_{Cmax} and J_{max} was reported by Farquhar et al. (1980). In this model, V_{Cmax25} (i.e. V_{Cmax} at 25°C) is calculated with superficial chlorophyll density (ρ_{chl}; assumed as 0.45 g m^{-2}), the turnover number of RuBP (carboxylase) (k_C; assumed as 2.5 s^{-1}), and the total CO_2 concentration of enzyme sites (E_t; assumed as 87.0 µmol g^{-1}. J_{max25} was computed as 467 times ρ_{chl} (Van Ooteghem, 2007). The calculated results of V_{Cmax25} and J_{max25} were 97.875 and 210.15 µmol m^{-2} s^{-1}, which are different from our predictions. These values lead to an overestimation of A_L (Model I). This underlines the insecure prediction quality of Model I and the central importance of carboxylation rate and maximum electron transport rate in photosynthesis prediction models.

For light-limited assimilation (A_j, electron transport-limited rate of photosynthesis), there are two widely used forms of the

equations, i.e. Eqns. 3 and 4. The rate of carboxylation when electron transport is limiting has not yet been described unambiguously in the FvCB model. As discussed by Yin et al. (2009b), for Eqn. 3, RuBP regeneration is assumed limited because of insufficient NADPH. Von Caemmerer (2000) elaborated that Eqn. 4 assumes ATP limiting: its two forms result from different assumptions about the operation of the Q cycle and the number of protons (H^+) required for synthesizing an ATP. Yin et al. (2009b) proposed that the stoichiometric relationship in Eqn. 4 assumes linear electron transport limited by ATP. Our results show a higher R^2 and lower RMSE with Eqn. 4, implying that in common production condition RuBP regeneration is likely limited by ATP. It can be deduced that under actual production conditions, ATP deficiency may be more related to RuBP regeneration limitation. (Qian et al., 2012), As there are some unknown pathways that cannot be fully represented by this model, the reverse cannot be supported by our data. The model discussed in this study, mainly concerns the basic circumstance (steady-state). A more robust model in unstable conditions could be the model proposed by Yin et al. (2004). However, with this model, constraints for the dynamic variables are needed.

Furthermore, when using Eqn. 10 to calculate the electron transport rate, the essential parameter is $\alpha_{(LL)}$. $\alpha_{(LL)}$ can be gained by mathematical curve fitting. Therefore, once $\alpha_{(LL)}$ is known, Eqn. 10 can be used to estimate the electron transfer rate in the absence of CFA.

In our model analysis, we have used real greenhouse data, in order to clearly interpret that a soft-sensor system can provide accurate information. In our simulations we used *ceteris paribus* conditions, as only one variable (CO_2 concentration) was changed, while the other potentially dynamic parameters were set fixed. However, as V_{Cmax} is an exponential function of light (Von Caemmerer and Edmondson, 1986; Brooks et al., 1988; Arulanantham et al., 1990; Makino et al., 1994; Qian et al., 2012; Qian et al., 2015), it should be emphasized that light condition need to be considered in the practical application. The next step would therefore include a full simulation study (including sensitivity analysis) varying all external variables. Due to the difficult parameterization process of NO_3^- reduction and its small contribution, the fraction of NO_3-used by ATP and NADPH was not considered in this study. However, in future investigations, this could be explored in hydroponics nutrient composition experiments variating NO_3^- or NH_4^+. This, nevertheless, was out of scope for the present research.

Our results suggest that (1) the CFA parameter Φ_2 can be used to predict net photosynthesis rate and that (2) a parameterized photosynthetic electron transport rate model is suitable to predict measured electron transport rate and leaf photosynthesis. The combination of CFA measurements and mathematical modelling can be used for plant performance monitoring and furthermore used as a module for a DSS. The model performance expressed as R^2 or RMSE was significantly improved with J_f.

Up-scaling A_L to A_{crop}, i.e. from leaf to canopy photosynthesis, will include the heterogeneity of vertical leaf differences in age and light adaptation resulting in leaf morphological differences (e.g. Laisk et al., 2005). For that it is necessary to estimate the model

parameters in A_L-predictions with different vertical distribution in the canopy.

To summarize, in the present paper the basis of a monitoring system was introduced, which combines chlorophyll fluorescence analysis and model predictions using a biochemical leaf photosynthesis model (Model II_b). The performance of a predictive model may be improved by combining it with the sensor-based on-line measurement of plant physiological parameters. The approach evaluated in this study provides information on the relationship between rates of photosynthetic electron transport and carbon gain. Furthermore, it could be used as the scientific basis for practical application of CO_2 enrichment in the greenhouse. The next step will be the incorporation of morphological differences of leaves in a canopy to the proposed soft-sensor system.

CONCLUSION

In summary, a soft-sensor, based on both sensors and models, is suitable to predicting rates of photosynthesis at the leaf level. However, for a well-fitting model system, a parameters validation of the biochemical parameters is needed. For estimating the CO_2 concentration in chloroplasts, coupling of the Jarvis model with Model I can avoid a vicious cycle of parameters. Model II_b could reduce the effects of the errors of the simplified model as indicated by the reduced R^2 between predicted data and measured data and the increased RMSE. Consequently, using these models as sub-systems in the soft-sensor approach could be a precise method for developing a greenhouse control strategy based on the direct evaluation of plant responses. However, differences in leaf morphology, which could result in different V_{Cmax} and J_{max} need to be exactly parameterized for a well performing DSS.

REFERENCES

Aggarwal, C., and Yu, S. (2005). An effective and efficient algorithm for high-dimensional outlier detection. *VLDB J.* 14, 211–221.

Allen, J. F. (2003). Cyclic, pseudocyclic and noncyclic photophosphorylation: new links in the chain. *Trends Plant Sci.* 8, 15–19.

Arulanantham, A. R., Rao, I. M., and Terry, N. (1990). Limiting Factors in Photosynthesis: VI. Regeneration of Ribulose 1,5-Bisphosphate Limits Photosynthesis at Low Photochemical Capacity. *Plant Physiol.* 93, 1466–1475.

Baker, N. R. (2008). Chlorophyll fluorescence: a probe of photosynthesis in vivo. *Annu. Rev. Plant Biol.* 59, 89–113.

Bernacchi, C. J., Pimentel, C., and Long, S. P. (2003). *In vivo* temperature response functions of parameters required to model RuBP-limited photosynthesis. *Plant Cell Environ.* 26, 1419–1430.

Björkman, O. (1973). Comparative studies on photosynthesis in higher plants. *Photophysiology* 8, 1–63.

Brooks, A., Portis, A. R., and Sharkey, T. D. (1988). Effects of Irradiance and Methyl Viologen Treatment on ATP, ADP, and Activation of Ribulose Bisphosphate Carboxylase in Spinach Leaves. *Plant Physiol.* 88, 850–853.

Chai, T., and Draxler, R. R. (2014). Root mean square error (RMSE) or mean absolute error (MAE)? – Arguments against avoiding RMSE in the literature. *Geosci. Model Dev.* 7 (3), 1247–1250.

Cornic, G., and Massacci, A. (1996). "Leaf photosynthesis under drought stress," in *Photosynthesis and the Environment*. Ed. N. R. Baker (Dordrecht: Kluwer Academic Publishers), 347–366.

Dannehl, D., Josuttis, M., Ulrichs, C., and Schmidt, U. (2014). The potential of a confined closed greenhouse in terms of sustainable production, crop growth, yield and valuable plant compounds of tomatoes. *J. Appl. Bot. Food Qual.* 87210 -, 219.

De Koning, A. N. M. (2006). Models and Sensors in greenhouse control. *Acta Horticuturae* 718, 175–182.

Dubois, J. J. B., Fiscus, E. L., Booker, F. L., Flowers, M. D., and Reid, C. D. (2007). Optimizing the statistical estimation of the parameters of the Farquhar-von Caemmerer-Berry model of photosynthesis. *New Phytol.* 176, 402–414.

Edwards, G. E., and Baker, N. R. (1993). Can CO2 assimilation in maize leaves be predicted accurately from chlorophyll fluorescence analysis? *Photosynth. Res.* 37 (2), 89–102.

Ethier, G., and Livingston, N. (2004). On the need to incorporate sensitivity to CO_2 transfer conductance into Farquhar – von Caemmerer – Berry leaf photosynthesis model. *Plant Cell Environ.* 27, 137–153.

Ethier, G. J., Livingston, N. J., Harrison, D. L., Black, T. A., and Moran, J. A. (2006). Low stomatal and internal conductance to CO2 versus Rubisco deactivation as determinants of the photosynthetic decline of ageing evergreen leaves. *Plant Cell Environ.* 29, 2168–2184.

Farquhar, G. D., and von Caemmerer, S. (1982). "Modelling of photosynthetic response to environmental conditions," in *Physiological Plant Ecology II, Water Relations and Carbon Assimilation. Encyclopedia of Plant Physiology, New Series*, vol. 12. B . Eds. O. L. Lange, P. S. Nobel, C. B. Osmond and H. Ziegler (Berlin, Germany: Springer Verlag), 549–588.

Farquhar, G. D., and Wong, S. C. (1984). An empirical model of stomatal conductance. *Aust. J. Plant Physiol.* 11, 191–209.

DATA AVAILABILITY STATEMENT

All datasets generated for this study are included in the article/ **Supplementary Material**.

AUTHOR CONTRIBUTIONS

WY performed the measurements. US was involved in planning and supervised the work. WY and OK processed the experimental data, performed the analysis, drafted the manuscript, and designed the figures. All authors discussed the results and commented on the manuscript.

FUNDING

ACKNOWLEDGMENTS

SUPPLEMENTARY MATERIAL

The Supplementary Material for this article can be found online at: https://www.frontiersin.org/articles/10.3389/fpls.2020.01038/full#supplementary-material

Farquhar, G. D., Von Caemmerer, S., and Berry, J. A. (1980). A biochemical model of photosynthetic CO_2 assimilation in leaves of C3 species. *Planta* 149, 78–90.

Farquhar, G. D., von Caemmerer, S., and Berry, J. A. (2001). Models of photosynthesis. *Plant Physiol.* 125, 42– 45.

Flexas, J., Briantais, J. M., Cerovic, Z., Medrano, H., and Moya, I. (1998). "Continuous chlorophyll fluorescence and gas exchange measurements as a new approach to study water stress effects on leaf photosynthesis," in Photosynthesis: Mechanisms and Effects, E. Garab, Ed., (Netherlands: Kluwer Academic), p. 4305–4308.

Flexas, J., Jean-Marie, B., Zoran, C., Hipólito, M., and Ismael, M. (2000). Steady-State and Maximum Chlorophyll Fluorescence Responses to Water Stress in Grapevine Leaves: A New Remote Sensing System. *Remote Sens. Environ.* 73, 283–297.

Flexas, J., Ribas-Carbo, M., Diaz-Espejo, A., Galmes, J., and Medrano, H. (2008). Mesophyll conductance to CO2: current knowledge and future prospects. *Plant Cell Environ.* 31, 602–621.

Flexas, J., Barbour, M. M., Brendel, O., Cabrera, H. M., Carriqui, M., Diaz-Espejo, A., et al. (2012). Mesophyll diffusion conductance to CO2: An unappreciated central player in photosynthesis. *Plant Sci.* 193-194, 70–84.

Foyer, C. H., and Noctor, G. (2002). Photosynthetic nitrogen assimilation and associated carbon and respiratory metabolism. *Photosynthetica* 41, 342.

Gijzen, H. (1992). *Simulation of photosynthesis and dry matter production of greenhouse crops* (Wageningen, The Netherlands: CABO-DLO).

Goudriaan, J., and Van Laar, H. H. (1994). *Modelling potential crop growth processes. vol. 2* (Dordrecht, The Netherlands: Kluwer academic publishers), 238 p.

Govindjee, E. (1995). Sixty-three years since Kautsky: Chlorophyll a fluorescence. *Aust. J. Plant Physiol.* 22, 131–160.

Grubbs, F. E. (1950). Sample criteria for testing outlying observations. *Ann. Math Statist* 21, 27–58.

Gurban, E. H., and Andreescu, G.-D. (2018). Greenhouse environment monitoring and control: State of the art and current trends. *Environ. Eng. Manage. J.* 17, 399–416.

Harley, P. C., and Sharkey, T. D. (1991). An improved model of C3 photosynthesis at high CO_2: reversed O2 sensitivity explained by lack of glycerate reentry into the chloroplast. *Photosynth. Res.* 27, 169–178.

Herppich, W. B., and Peckmann, K. (1997). Responses of gas exchange, photosynthesis, nocturnal acid accumulation and water relations of aptenia cordifolia to short-term drought and rewatering. *J. Plant Physiol.* 150 (4), 467–474.

Herppich, W. B., and Peckmann, K. (2000). Influence of drought on mitochondrial activity, photosynthesis, nocturnal acid accumulation and water relations in the CAM plants *prenia sladeniana* (ME-type) and *Crassula lycopodioides* (PEPCK-type). *Ann. Bot.* 86, 611–620.

Hoogenboom, G., Jones, J. W., and Boote, K. J. (1990). Modeling growth, development and yield of legumes: current status of the SOYGRO, PNUTGRO and BEANGRO models. *ASAE PaperNo., 90–1060 Paper presented at the ASAE International Summer Meeting*, Ohio, USA, 1990, 32 pp.

Herppich, W. B., Flach, B. M. T., von Willert, D. J., and Herppich, M. (1996). Field investigations of photosythetic activity, gas exchange and water potential at different leaf ages in Welwitschia mirabilis during a severe drought. *Flora* 191, 59–66.

Heuvelink, E. (1996). Tomato growth and yield: quantitative analysis and synthesis. [Ph.D. Thesis], Wageningen, The Netherlands: Wageningen Agricultural University.

Huber, C. (2011). *Bewertung des CO_2-Gaswechsels von ausgewählten Gemüsekulturen und Optimierung der Steuerung des CO_2-Gehaltes in semigeschlossenen Gewächshäusern.* [PhD thesis] (Germany: Humboldt Universitaet zu Berlin).

Janka, E., Körner, O., Rosenqvist, E., and Ottosen, C. O. (2013). High temperature stress monitoring and detection using chlorophyll a fluorescence and infrared thermography in chrysanthemum (Dendranthema grandiflora). *Plant Physiol. Biochem.* 67, 87–94.

Jones, J. W., Dayan, E., Allen, L H., van Keulen, H., and Challa Keulen, H. (1991). A dynamic tomato growth and yield model (TOMGRO). *T ASAE* 34, 663–672.

Körner, O., and Hansen, J. B. (2012). An on-line tool for optimising greenhouse crop production. *Acta Hortic.* 957, 147–154.

Körner, O., and Van Straten, G. (2008). Decision support for dynamic greenhouse climate control strategies. *Comput. Electron. Agric.* 60, 18–30.

Körner, O., Challa, H., and Van Ooteghem, R. J. C. (2002). Modeling temperature effects on crop photosynthesis at high radiation in a solar greenhouse. *Acta Hortic.* 593, 137–144.

Körner, O. (2004). Evaluation of crop photosynthesis models for dynamic climate control. *Acta Hortic.* 654, 295–302.

Körner, O. (2019). "Models, sensors and decision support systems in greenhouse cultivation," in *Achieving sustainable greenhouse cultivation*. Eds. L. F. M. Marcelis and E. Heuvelink (Burleigh Dodds: www.bdspublishing.com), 379–412.

Krall, J. P., and Edwards, G. E. (1992). Relationship between photosystem II activity and CO2 fixation in leaves. *Physiol. Plant.* 86 (1), 180–187.

Krause, G. H., and Weis, E. (1984). Chlorophyll fluorescence as a tool in plant physiology : II. Interpretation of fluorescence signals. *Photosynth Res.* 5, 139–157.

Laisk, A., Eichelmann, H., Oja, V., Rasulov, B., Padu, E., Bichele, I., et al. (2005). Adjustment of leaf photosynthesis to shade in a natural canopy: rate parameters. *Plant Cell Environ.* 28, 375–388.

Lattauschke, G. (2004). "Gewaechshaustomaten- Hinweis zum Umweltgerechten anbau und Managementunterlagen," in *Saechsische Landesanstalt fuer Landwirtschaft* (Dresden, Germany: Saechsisches Staatsministerium fuer Umwelt und Landwirtschaft).

Lawlor, D. W. (1995). "The effects of water deficit on photosynthesis", in Environment and Plant Metabolism. Ed. N. Smirnoff (Oxford: Bios Scientific Publishers), 129–160.

Lawlor, D. W., and Cornic, G. (2002). Photosynthetic carbon assimilation and associated metabolism in relation to water deficits in higher plants. *Plant Cell Environ.* 25, 275–294.

Leuning, R. (2010). A critical appraisal of a combined stomatal-photosynthesis model for C3 plants. *Plant Cell Environ.* 18, 339–355.

Lombardozzi, D. L., Smith, N. G., Cheng, S. J., Dukes, J. S., Sharkey, T. D., Rogers, A., et al. (2018). Triose phosphate limitation in photosynthesis models reduces leaf photosynthesis and gloval terrestrial carbon storage. *Environ. Res. Lett.* 13 (7), 1–9. doi: 10.1046/j.0016-8025.2001.00814.x

Long, S. P., and Bernacchi, C. J. (2003). Gas exchange measurements, what can they tell us about the underlying limitations to photosynthesis? Procedures and sources of error. *J. Exp. Bot.* 54, 2393–2401.

Madsen, K., Nielsen, H. B., and O, T. (2004). *Methods for non-linear least squares problems* (Lungby, Denmark: Technical University of Denmark), pp. 58.

Mahlein, A.-K. (2015). Plant disease detection by imaging sensors - Parallels and specific demands for precision agriculture and plant phenotyping. *Plant Dis.* 2, 241–251.

Makino, A., Nakano, H., and Mae, T. (1994). Effects of Growth Temperature on the Responses of Ribulose-1,5-Biphosphate Carboxylase, Electron Transport Components, and Sucrose Synthesis Enzymes to Leaf Nitrogen in Rice, and Their Relationships to Photosynthesis. *Plant Physiol.* 105, 1231–1238.

Manter, D. K., and Kerrigan, J. (2004). A/C$_i$ curve analysis across a range of woody plant species: influence of regression analysis parameters and mesophyll conductance. *J. Exp. Bot.* 55, 2581–2588.

Maxwell, K., and Johnson, G. N. (2000). Chlorophyll fluorescence–a practical guide. *J. Exp. Bot.* 51, 659–668.

Mehler, A. H. (1951). Studies on reactions of illuminated chloroplasts. I. Mechanism of the reduction of oxygen and other Hill reagents. *Arch. Biochem. Biophys.* 33, 65– 77.

Miflin, B. J. (1974). Nitrite reduction in leaves: studies on isolated chloroplasts. *Planta* 116, 187–196.

Miranda, L. (2017). *Artificial neural networks in greenhouse modelling-two modelling applications in horticulture.* [PhD thesis]. (Germany: Humboldt University).

Niinemets, U., Diaz-Espejo, A., Flexas, J., Galmes, J., and Warren, C. R. (2009). Importance of mesophyll diffusion conductance in estimation of plant photosynthesis in the field. *J. Exp. Bot.* 60, 2271–2282.

Nobel, P. S. (1977). Internal leaf area and cellular CO2 resistance: photosynthetic implications of variations with growth conditions and plant speciesm. *Physiol. Plant.* 40, 137–144.

Nobel, P. S. (1983). *Biophysical plant physiology and ecology* (San Francisco: W. H. Freeman and company).

Noctor, G., and Foyer, C. H. (1998). A re-evaluation of the ATP:NADPH budget during C3 photosynthesis: a contribution from nitrate assimilation and its associated respiratory activity? *J. Exp. Bot.* 49, 1895–1908.

Ögren, E., and Evans, J. R. (1993). Photosynthetic light-response curves. *Planta* 189, 182–190.

Orfanidis, S. J. (2006). "Introduction to Signal Processing", in *Fundamentals of protein NMR Spectroscopy*. Eds. R. S. Rule and H. T. Kevin. (The Netherlands: Springer), 65–88. doi: 10.1007/1-4020-3500-4

Pons, T. L., Flexas, S., von Caemmerer, S., Evans, J. R., Genty, B., Ribas-Carbo, M., et al. (2009). Estimating mesophyll conductance to CO₂: Methodology, potential errors and recommendations. *J. Exp. Bot.* 8, 8.

Qian, T., Elings, A., Dieleman, J. A., Gort, G., and Marcelis, L. F. M. (2012). Estimation of photosynthesis parameters for a modified Farquhar–von Caemmerer–Berry model using simultaneous estimation method and nonlinear mixed effects model. *Environ. Exp. Bot.* 82, 66–73.

Qian, T., Dieleman, J. A., Elings, A., de Gelder, A., and Marcelis, L. F. M. (2015). Response of tomato crop growth and development to a vertical temperature gradient in a semiclosed greenhouse. *J. Hortic. Sci. Biotechnol.* 90 (5), 578–584.

Ramin, S. R., Kalantari, F., C. Ting, K., R. Thorp, K., A. Hameed, I., Weltzien, C., et al. (2018). Advances in greenhouse automation and controlled environment agriculture: A transition to plant factories and urban agriculture. *Int. J. Agric. Biol. Eng.* 11, 1–22.

Robinson, J. M. (1987). "Interactions of carbon and nitrogen metabolism in photosynthetic and nonphotosynthetic tissues of higher plants: metabolic pathways and controls," in *Models in Plant Physiology and Biochemistry*, vol. 1. Eds. D. W. Newman and K. G. Wilson (Boca Raton, Florida USA: CRC Press), 25–35.

Rytter, M., Sørensen, J. C., Sørensen, B. N., and Körner, O. (2012). Advanced model-based greenhouse climate control using multi-objective optimization. *Acta Hortic.* 957, 29–35.

Salazar-Moreno, R., L.-C.I.L., Miranad, L., Schmidt, U., Fitz-Rodriguez, E., and Rojano-Aguilar, A. (2017). Development and validation of a dynamic climate model in a semiclosed greenhouse. *Acta Hortic.* 1182, 111–118. doi: 10.17660/ActaHortic.2017.1182.13

Schmidt, U. (1998). Low-cost system for on-line measurement of plant transpiration and photosynthesis in greenhouse production. *Acta Hortic.* 421, 249–257.

Schmidt, U. (2005). Microclimate control in greenhouse based on phytomonitoring data and mollier phase diagram. *Acta Hortic.* 691, 125–132.

Schreiber, U., Schliwa, U., and Bilger, W. (1986). Continuous recording of photochemical and non-photochemical chlorophyll fluorescence quenching with a new type of modulation fluorometer. *Photosynth. Res.* 10, 51–62.

Schreiber, U. (1986). *Detection of rapid induction kinetics with a new type of high-frequency modulated chlorophyll fluorometer* (Netherlands: Springer).

Schreiber, U. (2004). "Pulse-Amplitude (PAM) fluorometry and saturatio pulse method," in *chlorophyll a fluorescence. A signature of photosynthesis*. Ed. P. G. Govindjee (Dordrecht: Springer), 279–319.

Sharkey, T. D., Bernacchi, C. J., Farquhar, G. D., and Singsaas, E. L. (2007). Fitting photosynthetic carbon dioxide response curves for C3 leaves. *Plant Cell Environ.* 30, 1035–1040.

Sharkey, T. D. (1984). Transpiration-induced changes in the photosynthetic capacity of leaves. *Planta* 160, 143–150.

Sharkey, T. D. (1985). Photosynthesis in Intact Leaves of C₃ Plants: Physics, Physiology and Rate Limitations. *Bot. Rev.* 51, 53–105.

Shamshiri, R., Che Man, H., Zakaria, A. J., Beveren, P. V., Wan Ismail, W. I, and Ahmad, D. (2017). Membership function model for defining optimality of vapor pressure deficit in closed-field cultivation of tomato. *Acta Horticulturae* 1152, 281–290. doi: 10.17660/ActaHortic.2017.1152.38

Spitters, C. J. T., Van Keulen, H., and Van Kraalingen, D. W. G. (1989). "A simple and universal crop growth simulator: SUCROS87", in *Simulation and system management in crop protection*. Eds R. Rabbinge, S. A. Ward and H. H. Van Laar. 147–181. (Wageningen: Pudoc Wageningen), 147–181.

Sun, Y., Gu, L., Dickinson, R. E., Norby, R. J., Pallardy, S. G., and Hoffman, F. M. (2014). Impact of mesophyll diffusion on estimated global land CO2 fertilization. *Proc. Natl. Acad. Sci. U. States America* 111, 15774–15779.

Thornley, J. H. M. (1976). *Mathematical models in plant physiology[M]* (London, UK: Academic Press (Inc.)).

Tschiersch, H., Junker, A., Meyer, R. C., and Altmann, T. (2017). Establishment of integrated protocols for automated high throughput kinetic chlorophyll fluorescence analyses. *Plant Methods* 13, 1–16.

Tukey, J. W. (1977). *Exploratory data analysis* (Boston: Wesley Publishing Company).

Van Ooteghem, R. J. C. (2007). *Optimal control design for a solar greenhouse. PhD Thesis* (Wageningen, The Netherlands: Wageningen University).

Von Caemmerer, S., and Edmondson, D. (1986). Relationship between steady-state gas exchange, *in vivo* ribulose bisphosphate carboxylase activity and some carbon reduction cycle Intermediates in *Raphanus sativus*. *Aust. J. Plant Physiol.* 13, 669–688.

Von Caemmerer, S., and Farquhar, G. D. (1981). Some relationships between the biochemistry of photosynthesis and the gas exchange of leaves. *Planta* 153, 376–387.

Von Caemmerer, S. (2000). Biochemical Models of Leaf Photosynthesis. (Victoria, Australia: CISIRO Publishing), pp. 165.

Von Caemmerer, S. (2013). Steady-state models of photosynthesis. *Plant Cell Environ.* 36 (9), 1617–1630.

Walker, B. J., Strand, D. D., Kramer, D. M., and Cousins, A. B. (2014). The response of cyclic electron flow around photosystem I to changes in photorespiration and nitrate assimilation. *Plant Physiol.* 165 (1), 453–462.

Wallach, D., Wallach, D., Makowski, D., and Jones, J. W. (2006). *Working with dynamic crop models evaluation, analysis, parameterization, and applications* (Amsterdam: Elsevier), 11–54.

Warren, C. (2006). Estimating the internal conductance to CO₂ movement. *Funct. Plant Biol.* 33, 431–442.

Woodrow, I. E., and Berry, J. A. (1988). Enzymatic regulation of photosynthetic CO₂ fixation in C₃ plants. *Ann. Rev. Plant Physiol. Plant Mol. Biol.* 39, 533–594.

Yin, X., and Struik, P. C. (2009). Theoretical reconsiderations when estimating the mesophyll conductance to CO₂ diffusion in leaves of C3 plants by analysis of combined gas exchange and chlorophyll fluorescence measurements. *Plant Cell Environ.* 32, 1513–1524.

Yin, X. Y., and Struik, P. C. (2012). Mathematical review of the energy transduction stoichiometries of C4 leaf photosynthesis under limiting light. *Plant Cell Environ.* 35, 1299–1312.

Yin, X., Van Oijen, M., and Schapendonk, A. (2004). Extension of a biochemical model for the generalized stoichiometry of electron transport limited C3 photosynthesis. *Plant Cell Environ.* 27, 1211–1222.

Yin, X., Harbinson, J., and Struik, P. C. (2006). Mathematical review of literature to assess alternative electron transports and interphotosystem excitation partitioning of steady-state C₃ photosynthesis under limiting light. *Plant Cell Environ.* 29, 1771–1782.

Yin, X., Struik, P. C., Romero, P., Harbinson, J., Evers, J. B., Pe, V. D. P., et al. (2009a). Using combined measurements of gas exchange and chlorophyll fluorescence to estimate parameters of a biochemical C3 photosynthesis model: a critical appraisal and a new integrated approach applied to leaves in a wheat (Triticum aestivum) canopy. *Plant Cell Environ.* 32, 448–464.

Yin, X., Harbinson, J., and Struik, P. C. (2009b). "A model of the generalised stoichiometry of electron transport limited C₃ photosynthesis: development and application," in *Photosynthesis in Silico. Understanding Complexity from Molecules to Ecosystems*. Eds. A. Laisk, L. Nedbal and Govindjee, (Dordrecht, Netherlands: Springer), 247– 273.